frontiers in Chemical Engineering

ORIGINAL RESEARCH
published: 30 November 2021
doi: 10.3389/fceng.2021.765457

Electrochemical Ammonia: Power to Ammonia Ratio and Balance of Plant Requirements for Two Different Electrolysis Approaches

Jessica Allen[1]*, *Sebastien Panquet*[1,2] *and Adrian Bastiani*[2]

[1]School of Engineering, University of Newcastle, Callaghan, NSW, Australia, [2]Restech Pty Ltd., University of Newcastle, Callaghan, NSW, Australia

Electrochemical ammonia generation allows direct, low pressure synthesis of ammonia as an alternative to the established Haber-Bosch process. The increasing need to drive industry with renewable electricity central to decarbonisation and electrochemical ammonia synthesis offers a possible efficient and low emission route for this increasingly important chemical. It also provides a potential route for more distributed and small-scale ammonia synthesis with a reduced production footprint. Electrochemical ammonia synthesis is still early stage but has seen recent acceleration in fundamental understanding. In this work, two different ammonia electrolysis systems are considered. Balance of plant (BOP) requirements are presented and modelled to compare performance and determine trade-offs. The first option (water fed cell) uses direct ammonia synthesis from water and air. The second (hydrogen-fed cell), involves a two-step electrolysis approach firstly producing hydrogen followed by electrochemical ammonia generation. Results indicate that the water fed approach shows the most promise in achieving low energy demand for direct electrochemical ammonia generation. Breaking the reaction into two steps for the hydrogen fed approach introduces a source of inefficiency which is not overcome by reduced BOP energy demands, and will only be an attractive pathway for reactors which promise both high efficiency and increased ammonia formation rate compared to water fed cells. The most optimised scenario investigated here with 90% faradaic efficiency (FE) and 1.5 V cell potential (75% nitrogen utilisation) gives a power to ammonia value of 15 kWh/kg NH_3 for a water fed cell. For the best hydrogen fed arrangement, the requirement is 19 kWh/kg NH_3. This is achieved with 0.5 V cell potential and 75% utilisation of both hydrogen and nitrogen (90% FE). Modelling demonstrated that balance of plant requirements for electrochemical ammonia are significant. Electrochemical energy inputs dominate energy requirements at low FE, however in cases of high FE the BOP accounts for approximately 50% of the total energy demand, mostly from ammonia separation requirements. In the hydrogen fed cell arrangement, it was also demonstrated that recycle of unconverted hydrogen is essential for efficient operation, even in the case where this increases BOP energy inputs.

Keywords: electrochemical ammonia, balance of plant, power to ammonia, process model, electrochemical process, scale-up

OPEN ACCESS

Edited by:
Richard G. A. Wills,
University of Southampton,
United Kingdom

Reviewed by:
Yusuf Bicer,
Hamad bin Khalifa University, Qatar
Manoj Neergat,
Indian Institute of Technology
Bombay, India

***Correspondence:**
Jessica Allen
j.allen@newcastle.edu.au

Specialty section:
This article was submitted to Electrochemical Engineering, a section of the journal Frontiers in Chemical Engineering

Received: *27 August 2021*
Accepted: *03 November 2021*
Published: *30 November 2021*

Citation:
Allen J, Panquet S and Bastiani A (2021) Electrochemical Ammonia: Power to Ammonia Ratio and Balance of Plant Requirements for Two Different Electrolysis Approaches. Front. Chem. Eng. 3:765457. doi: 10.3389/fceng.2021.765457

1 INTRODUCTION

Large-scale production of synthetic ammonia has become one of the most important industries supporting the human population. It is theorised that ammonia-based fertilisers have enabled the global population to be at least 2 to 3 billion more people due to the increase in mass produced food crops from the use of these fertilisers in agriculture (Erisman et al., 2008). Ammonia also has many uses besides fertiliser. It is often made into ammonium nitrate explosives for mining, intermediate chemicals for pharmaceutical synthesis, cleaning agents and commercial refrigerants. Its global use has led to more than 175 million tonnes being produced annually, with an estimated 451 million tons of carbon dioxide emissions, accounting for 1% of the global emissions (Boerner, 2019). Recently, interest in ammonia as a fuel to decarbonise global shipping has gained some popularity and the ammonia economy has been suggested as an important option more broadly in global decarbonisation (MacFarlane et al., 2020). Since shipping accounts for approximately 1.7% of global emissions, green ammonia will be able to have significant impact (Ritchie and Roser, 2020).

Ammonia generation has remained largely unchanged since its inception in the mid-19th century, using steam-methane reforming followed by the Haber-Bosch process. Ammonia forms from hydrogen and nitrogen gas, **Eq. 1** below. Ammonia synthesis is exothermic so a higher temperature reactor will decrease the kinetics of the reaction overall, the reactors having staged cooling and catalyst beds to limit temperature rise and allow for maximized conversion opportunities.

$$3H_{2(g)} + N_{2(g)} \leftrightarrow 2\,NH_{3(g)} \tag{1}$$

Products are favored under high pressures and, in practice, ammonia synthesis occurs at high pressure (120–300 bar) and moderately high temperature (350–500°C) with low overall conversion (Rouwenhorst et al., 2019). The ammonia is separated by refrigeration/condensation before the remaining reactants are recycled, operating with typically less than 20% conversion through the main reactor and with substantial recycle flows (Rouwenhorst et al., 2019). In order to provide hydrogen to the process, natural gas is traditionally used and acts as to both produce hydrogen feedstock as well as being directly combusted for process heat. Typical energy demands for commercial plants are 30–35 GJ/tonne NH_3 (8.3–9.7 kWh/kg NH_3) with compression and hydrogen production occupying the bulk of the energy inputs (Smith et al., 2020).

Decarbonising ammonia generation could proceed in a number of ways. Hydrogen can be supplied by water electrolysis rather than through natural gas reforming, replacing natural gas derived hydrogen in the traditional Haber-Bosch process. Other process modifications include the need for electrically driven heating and handling energy fluctuations required for renewables integration. Energy requirements are not expected to be substantially larger when integrating with renewables, electrically driven plants suggested to require 40–45 GJ/t_{NH3} (11.1–12.5 kWh/kg NH_3) (Smith et al., 2020). Replacing existing emission intensive operations however would require substantial new investment in renewable electricity, preferably in managed industrial precincts allowing for security of both supply and reducing cost of infrastructure to supply renewable electricity to site.

Alternatively, smaller and more distributed ammonia production could be considered. This approach is gaining research popularity in recent years to optimise renewable technology integration. Process design of the Haber-Bosch demonstrates increased energy demand at small scales due to heat losses which dominate in smaller equipment items (Rouwenhorst et al., 2019), however the idea of decentralised ammonia production from local resources (like air and water) is an attractive concept gaining traction (Palys et al., 2018; Rouwenhorst et al., 2019; Smith et al., 2020; Chehade and Dincer, 2021; Yoshida et al., 2021).

It is possible to synthesise ammonia at significantly reduced temperature and pressure, via an electrochemical route, side-stepping the Haber-Bosch process entirely. This involves a system in which the feedstock enter a cell and are converted electrochemically to ammonia by forcing the movement of electrons while the reactants contact the surface of catalysts affixed to conductive electrodes. This condition change could mean a large energy saving in terms of heating or pressurising on a large scale, and a more streamlined and potentially safer integration into an industrial ammonia process. Like the modern small-scale Haber-Bosch approach, the hydrogen used for the electrochemical synthesis can be sourced by renewable powered water electrolysis and the overall reaction identical to **Eq. 1**. Some cells alternatively have the potential to perform this conversion *in-situ*, eliminating an extra step and directly being fed water. Ammonia generation using water as a reactant is shown in **Eq. 2**:

$$3H_2O + N_2 \leftrightarrow 2\,NH_3 + 3/2O_2 \tag{2}$$

Using water as a proton source means more work needs to be done within the electrochemical ammonia synthesis reactor, demanding more energy than the hydrogen fed electrolysis unit. However the hydrogen fed approach also needs initial water electrolysis to produce decarbonised hydrogen as a feedstock to the process.

In terms of electrochemical reduction of nitrogen, attempts to date find that large overpotentials are required, with low production rates of ammonia (Giddey et al., 2013; Singh et al., 2017; Tang and Qiao, 2019; Xue et al., 2019) and the technology readiness of this route is still low (Rouwenhorst et al., 2019). The electrochemical selectivity towards ammonia is often low, due to competing hydrogen evolution reaction resulting in low faradaic/current efficiency. As a result of the difficulty in both fixation and transformation of nitrogen gas, electrochemical synthesis methods are widely varied for ammonia production and include liquid electrolytes near room temperature, molten salt electrolytes at intermediate temperature, solid electrolytes with wide operating temperature (generally high temperature), and composite electrolytes (solid electrolytes and low melting point salt)—all of which have been exhaustively studied and findings

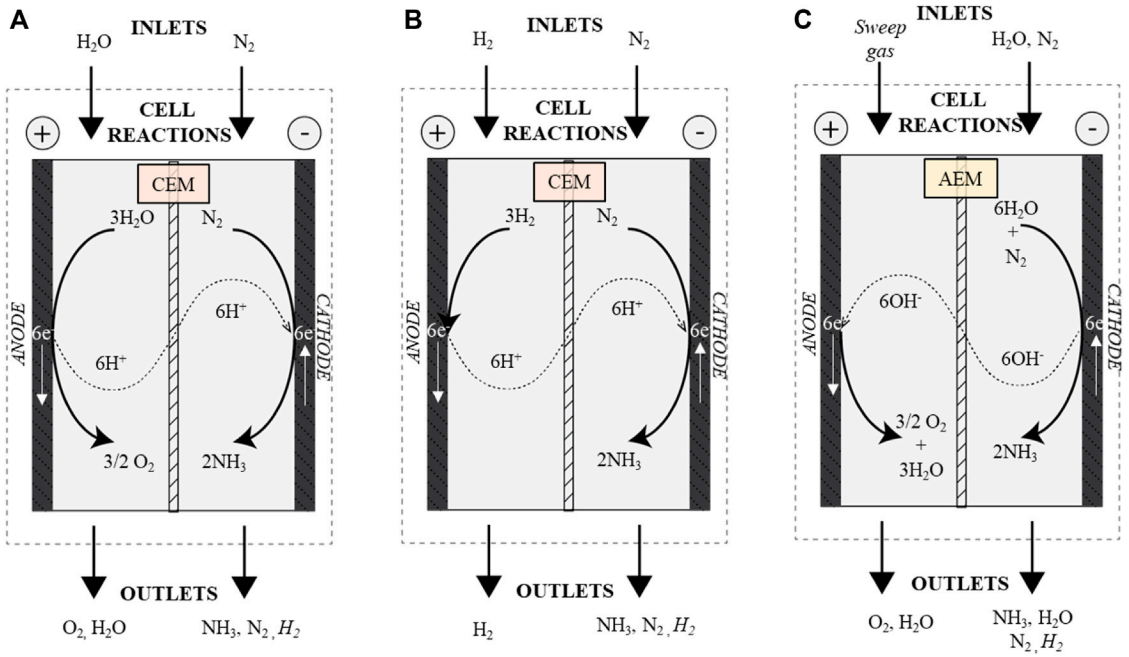

FIGURE 1 | Cell arrangements for electrochemical ammonia synthesis including anodic and cathodic reaction paths **(A)** water fed cell (H_2O-fed) using a cation exchange membrane (CEM) **(B)** hydrogen fed (H_2-fed) cell using a CEM and **(C)** water fed cell (H_2O-fed) using an anion exchange membrane (AEM).

collated (Amar et al., 2010; Lan et al., 2013; Kyriakou et al., 2017; Shipman and Symes, 2017; Zhou et al., 2017; Xue et al., 2019; MacFarlane et al., 2020; Yang et al., 2020). The reaction pathways for the cathode and anode are similarly diverse and a variety of membranes and ion transfer approaches have been attempted with mixed success. A schematic of major reaction pathways and expected inputs and outputs in flow-through cell arrangements are outlined in **Figure 1**.

Three main reaction pathways can be explored with either water fed (H_2O-fed) (**Figures 1A,C**), or hydrogen fed (H_2-fed) (**Figure 1B**) reactants including either a cation (CEM) or anion (AEM) exchange membrane. Many investigations concentrate solely on the ammonia evolution reaction (anodic cell), providing protons through acidic conditions and aqueous solutions. There are also several promising set-ups using mediated reaction pathways including recent results of Cherepanov et al. (2021). While the AEM approach has shown some promise, investigations are more limited and the input/outputs for this arrangement are significantly different and will not be considered further here.

In terms of the overall performance, there is a balance to be found in faradaic efficiency (also referred to as current efficiency) and the ammonia production rate. The faradaic efficiency represents the proportion of total charge passed through the cell that results in the generation of the intended product, the most likely reason for a low efficiency being the formation of hydrogen rather than ammonia at the cathode. The ammonia production rate is the rate of ammonia formed normalised on a time basis and usually over the geometric electrode area, although some authors prefer to normalise based on the catalyst loading of a particular cell. This is a popular comparison to make in the literature with several works plotting efficiency versus area normalised ammonia evolution rate, although no clear trend has been observed between the two variables. Tang and Qiao (2019) observed improvements in both values reported on over a short 3 year period, Wu et al. (2021) provided a materials focused comparison while Shipman and Symes (2017) and Kyriakou et al. 2017) collated early results. More recently Choi et al. (2020) listed over 120 papers published between 2010 and 2020 where several method based errors in reporting rates and efficiency were highlighted, going some way to explain huge variation and limited agreement between findings.

Focusing on cell arrangements where a CEM with proton transfer and either water or hydrogen proton sources at room temperature, outcomes for faradaic efficiency versus ammonia formation rate are compared in **Figure 2A**.

For the same studies, the theoretical cell potential has also been calculated from the half-cell reaction potential measured, as shown in **Figure 2B**. The theoretical cell voltage at room temperature for **Eq. 2** is 1.17 V while **Eq. 1** is theoretically spontaneous at room temperature (<0 V), meaning it might be expected to generate energy like a fuel cell when the circuit is connected ($E_{t,H2}$ = +0.056 V, see **Figure 2C**). In practice, no spontaneous ammonia formation has been observed in the literature. In the work of Lan et al., no ammonia generation was observed for a hydrogen fed cell until at least 0.2 V was externally applied (Lan et al., 2013), while substantial rates were not seen until an applied voltage of 0.4 V or greater. The large overpotential of ammonia formation means that at least some applied potential is required with the majority of half-cell

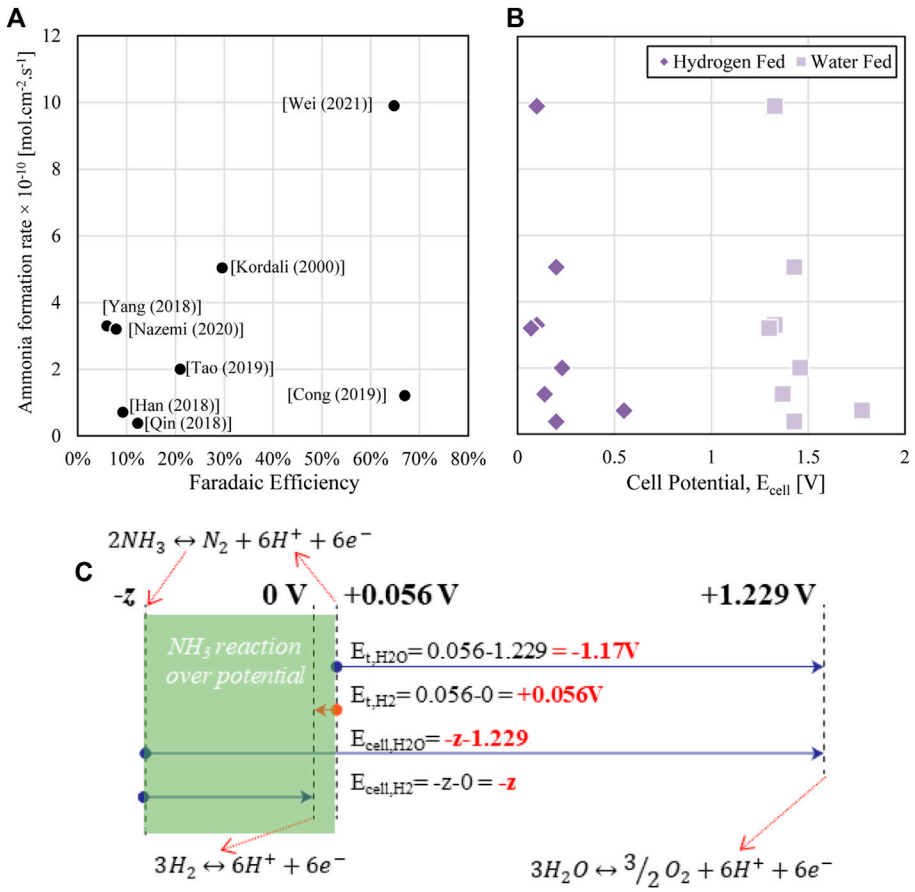

FIGURE 2 | (A) Reported performance from selected studies (Kordali et al., 2000; Han et al., 2018; Qin et al., 2018; Yang et al., 2018; Cong et al., 2019; Tao et al., 2019; Nazemi et al., 2020; Wei et al., 2021) of faradaic efficiency and ammonia formation rate, **(B)** theoretical full cell potential for reported literature half-cell and relationship to ammonia formation rate [*y*-axis same as **(A)**] **(C)** schematic representation of cell potential calculation in impact of ammonia formation overpotential in V vs NHE (normal hydrogen electrode) where $E_{t,\ H2O}$ and $E_{t,H2}$ represent the theoretical potential for a reaction generating ammonia from either water or hydrogen as the proton source while $E_{cell,H2}$ and $E_{cell,H2O}$ represent the measured potential required for the full cell arrangement which has 'z V' overpotential.

investigations showing a negative cell potential for ammonia generation. **Figure 2B** shows the indicative cell potential (reported as a positive value) reported in literature, where E_{cell} of a water fed cell is $[E_{cell,H_2O} = -z - 1.229]$ and E_{cell} of a hydrogen fed cell is $[E_{cell,H_2} = -z]$, where z is the reported potential of ammonia evolution versus the normal hydrogen electrode (NHE), as shown schematically in **Figure 2C**. There is no clear relationship between the cell potential and ammonia evolution rate in **Figure 2B**, although higher potentials tend to decrease the evolution rate.

Total cell voltage is not always reported in the literature and in fact many authors report specifically on half-cell results, focusing on the ammonia evolution reaction and usually reported versus the normal hydrogen electrode (NHE). In practice, overpotentials and internal cell resistances will mean that at least some additional applied voltage on top of the half-cell value will be required for a full cell evolving both oxygen and ammonia, meaning estimates in **Figure 2B** are likely lower than real cells. The full cell voltage will depend on the final arrangement of the electrolyser including membrane and flow assembly.

The faradaic efficiency and operating voltage are linked to the energy requirements of the electrolyser, while the ammonia yield rate is an indication of the effective size of active electrode area required, or in some cases catalyst quantity that would be required for a set ammonia yield. Larger cells often indicate high equipment and catalyst costs and unrealistic plant footprints. The US department of energy has set targets of 90% faradaic efficiency with an evolution rate of 10^{-6} mol s^{-1} cm^2. This has not yet been achieved in the literature although consistent improvements have been observed.

Indeed the technology is early stage, very few authors progressing beyond bench scale and even half-cell reactions towards a full electrochemical synthesis with integrated in and out flows. Issues with experimental validity and reproduction of results have also been encountered, as outlined by MacFarlane et al. (2020), although some recent breakthroughs in increased faradaic efficiency and ammonia production rate could point towards redox mediated approaches as being more promising moving forward (Suryanto et al., 2021).

While half-cell and small scale electrochemical ammonia reactors have been investigated in detail, little focus has been

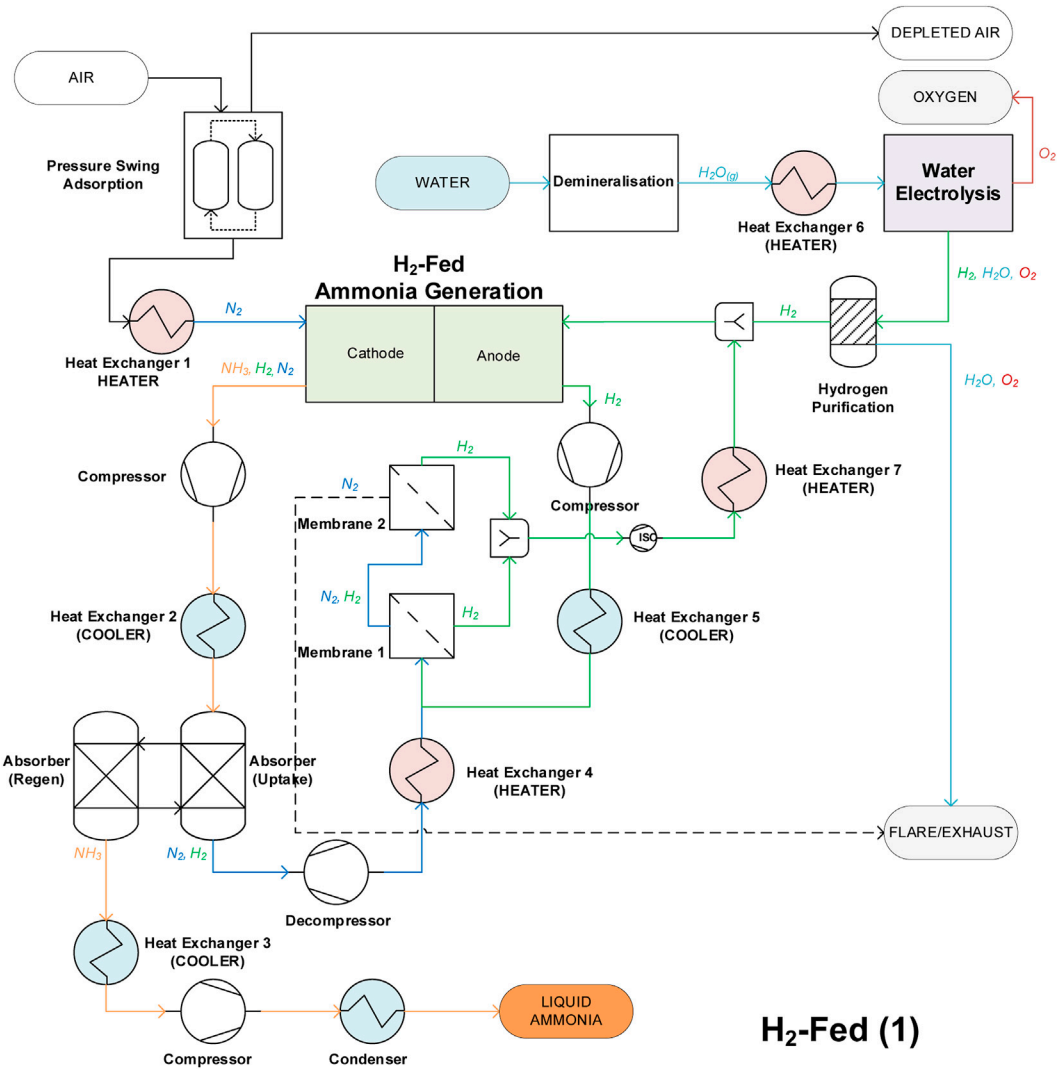

FIGURE 3 | Hydrogen-fed process flow arrangement [H_2-fed (1)] including anode stream recycle.

on the practical application and process integration of these units. Even at this early stage, the overall process design deserves consideration. The balance of plant (BOP) equipment and overall process energy demands could influence the viability of a given cell. This is particularly true when the underlying conditions and mixtures of gases and liquids varies widely in the electrochemical application compared to the existing commercial application.

Kugler et al. generated an ASPEN based model of the water fed process, using the custom modeler for the electrochemical component (Kugler et al., 2014). The optimised single pass system, based on performance values far beyond those currently achievable and >80% faradaic efficiency, predicted a power to ammonia value of 11.36 kWh/kg NH_3 with very minor contribution calculated from the balance of plant. Other high level assessments of electrical energy demands have also been attempted in order to broadly assess the potential of electrochemical approaches compared to traditional Haber-Bosch, reporting values of 7.5–11 kWh/kg NH_3, although it is unlikely these values considered the balance of plant (Rouwenhorst et al., 2019).

In this work, three preliminary arrangements for electrochemical ammonia generation are presented. Their process energy demands are estimated using known performance data, first principles thermodynamics and high level performance data. The focus is on overall power inputs and key sensitivities in order to understand potential challenges in up-scaling the process once fundamental constraints are met. These include the extent of reactant conversion, faradaic efficiency and energy demand of the cell as well as the impact of recycle streams. Key separation steps are also highlighted since the conditions and combinations of species in each stream are often different to what is seen in a commercial ammonia chemical synthesis plant and may require additional fundamental development.

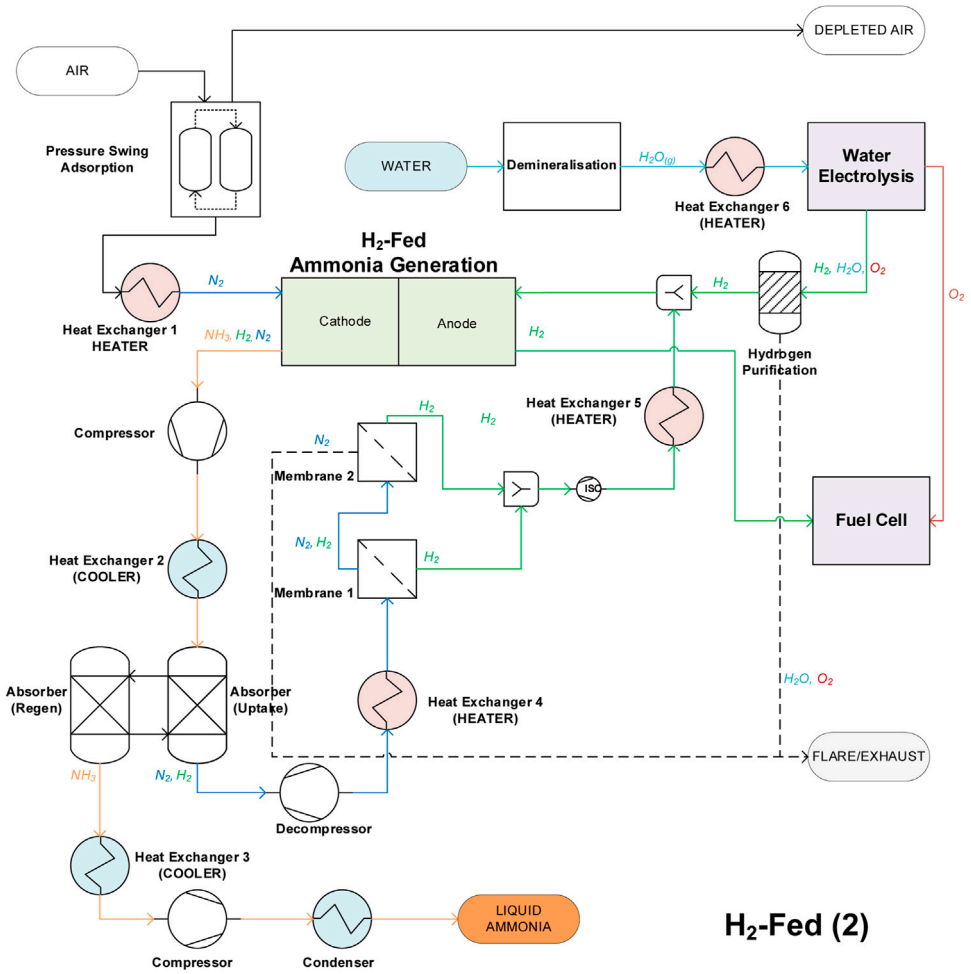

FIGURE 4 | Hydrogen-fed process flow arrangement [H_2-fed (2)] without anode hydrogen recovery.

2 MODEL DETAILS

In this work, cell arrangements are separated into either water-fed (H_2O-fed) or hydrogen fed (H_2-fed) with consideration of proton exchange only. Variations from this (such as the AEM shown in **Figure 1**) will have different mixtures of reactants and would require alternate process arrangements. Focus is on process flow analysis and high level requirements, not detailed modelling of individual unit operations. A similar modelling approach was used previously for the high temperature direct carbon fuel cell, a technology also at a low overall technology readiness level (Allen et al., 2020). Process flowsheets showing main unit operations for the hydrogen fed (**Figures 3**, **4**) and water fed (**Figure 5**) systems.

A model has been built integrating system components using assumptions outlined in this section, unit operations are assumed to be adiabatic and gases have been assumed to be ideal, although compressibility factor was used in compression calculations. Many components are common to both arrangements while some unit operations are specific to either water or hydrogen fed cells. In all models, the cathode side of the ammonia synthesis is identical. This includes nitrogen production for feed to the ammonia synthesis, followed by compression and ammonia separation. The gas component then undergoes additional separation steps to recover hydrogen generated as a by-product at the anode, although some nitrogen is still expected to be present. In the hydrogen fed approach, hydrogen from the cathode is recycled to the anode side of the ammonia synthesis cell. In the water fed approach, this hydrogen is directed towards a fuel cell for energy recovery since it cannot be reused within the water fed cell.

The anode side in all approaches includes an initial demineralization/water purification step where the purified water is fed to either a water electrolysis unit (H_2-fed cells) or directly to the ammonia synthesis (H_2O-fed cell). In the H_2O-fed cell, unconverted water is separated from the oxygen gas product. The water is recycled to the ammonia synthesis and the oxygen is fed to the fuel cell. For the H_2-fed approach following water electrolysis the hydrogen generated is purified and dried before being introduced to the ammonia synthesis step. Unconverted hydrogen cannot be directly recycled back to the ammonia synthesis reactor as the recycle of the cathode stream results in the small amount of nitrogen present after membrane

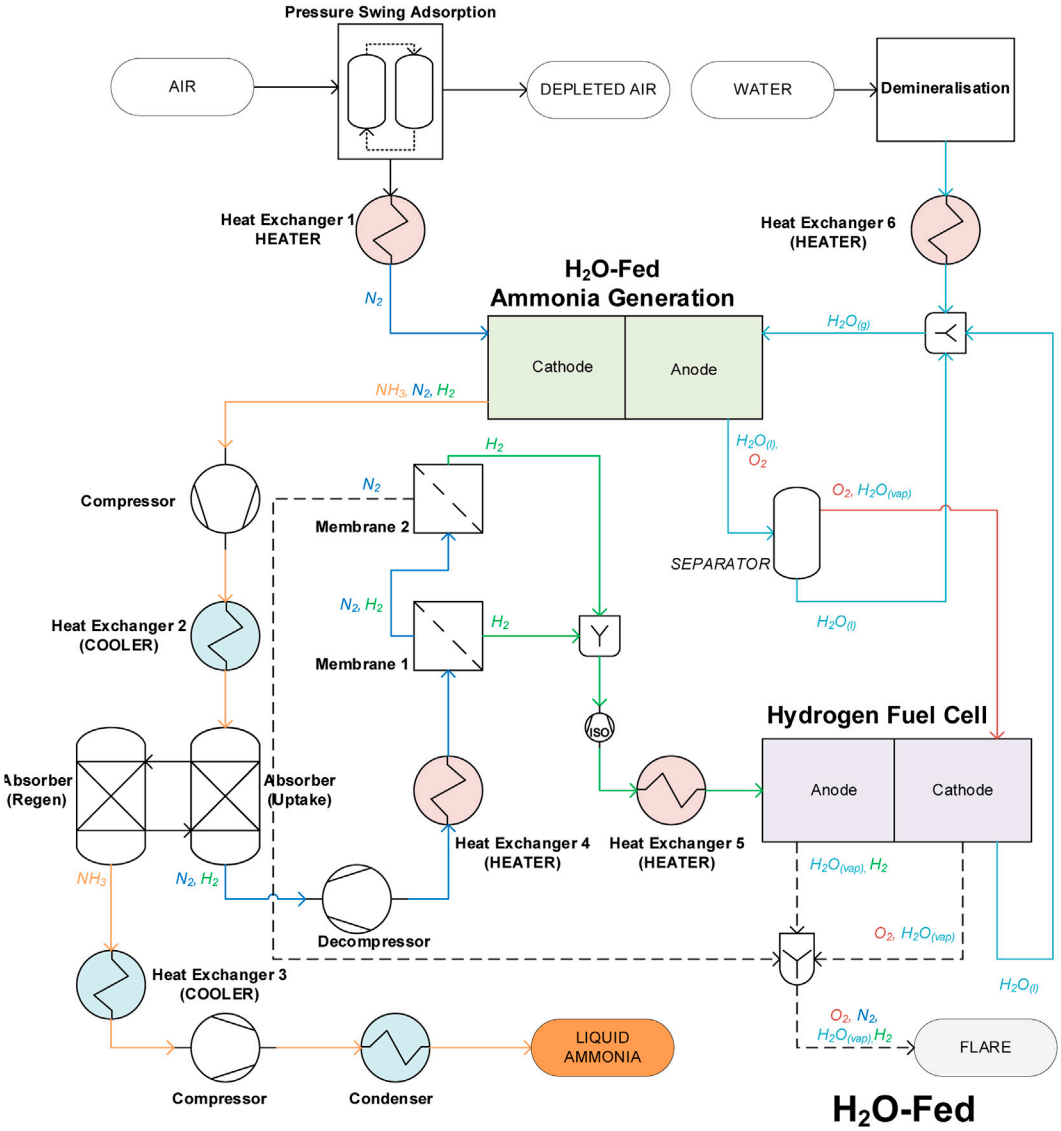

FIGURE 5 | Water fed cell process flow arrangement (H_2O-fed).

separation. If this stream was continuously recycled nitrogen would build up in the reactor. Instead this stream can either be redirected through the membrane along with the anode recycle stream or utilised in an external fuel cell for energy recovery. Both options are considered here with H_2-fed (1) being the recycle option and H_2-fed (2) using the fuel cell offset.

2.1 Nitrogen Production

Nitrogen production techniques were recently reviewed by Sánchez and Martín (2018) who determined cryogenic air separation was still the preferred method for large scale plants in terms of both cost and energy requirements. However as the scale of production reduces, both membrane and pressure swing adsorption (PSA) should be considered. PSA was outlined as the best choice for small to moderate scale operations recently by Rouwenhorst et al. with nitrogen purity of 99.8wt% achievable (0.001 wt% oxygen) using energy consumption of approximately 0.3 kWh/kg N_2 produced (Rouwenhorst et al., 2019). It was suggested that additional oxygen separation would be required, however this applies to the Haber-Bosch process where oxygen acts to poison reactor catalysts. In electrochemical ammonia generation, oxygen is not deemed problematic, in fact several studies also investigating performance using air as a nitrogen source (Lan et al., 2013; Shipman and Symes, 2017). **Supplementary Table S1** outlines all input assumptions used for PSA calculations in this work.

2.2 Heat Exchangers (Utilities)

For both hydrogen and water fed approaches heat exchangers are required to control streams to specific reactor conditions. Heat exchangers are also required after gas compression to reduce temperature gains. Overall process utility requirements were calculated for this work using systematic 1st and 2nd law

thermodynamics heat exchange principles, also known as pinch analysis, to determine final utility requirements after optimised internal process energy use (exchange between process streams). Pinch temperatures of 10°C were used, following the method of Kemp (2011), although a full heat exchanger network design was not completed. Enthalpy change in each stream was calculated as outlined in Allen et al. (2020) with specific properties of streams (heat capacity) used in this work detailed in **Supplementary Tables S2, S3**.

2.3 Compression/Decompression

Polytropic compression (polytropic efficiency, η_{poly} = 70%) using electrical efficiency of η_{elec} = 75% was used (Palys et al., 2018; Smith et al., 2020). Outlet temperature of compressed gases (used for compression and decompression) and compressor work ($\dot{W}_{comp}$) were calculated using **Eqs 3–5**, gas properties from **Supplementary Tables S2, S3** and heat capacity ratios from **Supplementary Table S4**.

$$T_{out} = T_{in}\left(\frac{P_{out}}{P_{in}}\right)^{\frac{n-1}{n}} \tag{3}$$

$$\frac{n-1}{n} = \frac{1}{\eta_{poly}}\frac{\gamma-1}{\gamma} \tag{4}$$

$$\dot{W}_{comp} = \dot{m}\frac{n}{(n-1)\eta_{elec}\eta_{poly}}\frac{z_{in}RT_{in}}{MW_{gas}}\left[\left(\frac{P_{out}}{P_{in}}\right)^{\frac{n-1}{n}} - 1\right] \tag{5}$$

Where T_{in} and T_{out} are inlet and outlet gas temperatures (K), P_{in} and P_{out} are inlet and outlet pressure (kPa), $\dot{m}$ is the mass flow rate (kg/s) and R the ideal gas constant. Mass weighted average for the molecular weight (MW_{gas}) and compressibility factor (z_{in}) of gases was used (at inlet conditions). η_{poly} and η_{elec} are the polytropic and electrical efficiency of the compressors.

Decompression was only used in the case of reducing pressure from 20 to 3 bar, and assumed to proceed via pressure let down. The same equations (**Eqs 3–4**) were used to calculate stream temperature changes, and no energy was ascribed to this operation. Isothermal expansion was assumed in the small pressure change from 3 to 1 bar following the membrane separation units. Isothermal expansion includes the application of a load to force the expanding gas to do work, therefore generating heat and enabling a consistent temperature where the pressure release would normally lead to cooling.

2.4 Condensers

Energy used to change the temperature and phase of specific streams was used to calculate theoretical thermal heat rejection required to reduce the temperature of gas streams to the liquid phase. This occurs while under increased pressure for ammonia condensation following the adsorption step. The enthalpy of phase change was taken at the product compressor outlet condition of 23.4 bar (see **Section 2.10**), which results in a boiling point of ~45°C and enthalpy of phase change of 1,073 kJ/kg [fundamental data used from (Don and Robert, 2008)].

2.5 Membrane Separation

The membrane separation unit allows for purification of hydrogen generated at the cathode (through inefficiency) which can then be either recycled to the anode (hydrogen-fed system, option 1) or utilised to generate electrical energy in a hydrogen fuel cell (water-fed system). In the case of the H2-fed (1) cell and the recycle loop used, the membrane system also provides an exit for other species entering the loop via the PSA unit. In both systems, the retentate of the membrane system, which is mostly nitrogen with some argon and unseparated hydrogen, is exhausted through a flare to remove this build up.

Specialised membranes such as polyimide Matrimid® 5218, applied at scale as asymmetric hollow-fibers, are capable of this separation and are semi-tolerant of the ammonia that would be present in the gas phase (Schell, 1985; David et al., 2011; David et al., 2012), although in practice this would likely be scrubbed out to avoid possible contamination or membrane degradation. These membranes have been tested and documented on many gas separations including the hydrogen-nitrogen mix in ratios of 20/80, 50/50, and 80/20 vol%. The data provided by David et al. (David et al., 2011; David et al., 2012) shows that for an operating temperature of 20°C and inlet pressure between 2 to 6 bar, the membrane operated as shown in **Supplementary Table S5**. In order to maintain the accuracy when performing calculations around the membrane units, the inlet temperature was kept at 30°C in this work, however the membrane can handle operation up until its glass transition point at approximately 300°C, so cooling after the compressor may be reduced in practice. This may also impact on the maximum allowable pressure however and has not been considered here.

A mid-range pressure of 3 bar was used in this work with final hydrogen grade produced at 99.18 mol% (nitrogen balance) (David et al., 2012) and a recovery of 88.5 mol% per pass (Schell, 1985). Energy requirements were constrained to the compression required to bring the inlet to required pressure, as calculated in **Section 2.3**, while decompression prior to final use of the post-membrane stream was included as an isothermal decompression.

2.6 Hydrogen Purification (H_2-Fed Cell Only)

To avoid build-up of both oxygen and water vapour in the hydrogen recycle of the anode compartment in the hydrogen-fed systems, removal of both contaminants are required. This is also an issue for green ammonia plants where the hydrogen generated must be sent through the Haber-Bosch reactor which is highly sensitive to oxygen containing species. Removal of both oxygen and water is also a consideration for small scale electrolysis where hydrogen is being generated for energy storage purposes, since fuel cell grade hydrogen has highly specified low concentrations of oxygen and water (Ligen et al., 2020).

Industrial practice specifies a deoxygenation reactor (Peschel, 2020) which catalytically combines hydrogen with oxygen to generate additional water in an exothermic reaction. In this work the inlets are fed at electrolysis temperature of 60°C before entering the adiabatic reactor and reducing oxygen concentration to 1 ppmV, also consuming hydrogen and generating additional water vapour in line with the reaction: $2H_2 + O_2 \rightarrow 2H_2O$.

Drying the hydrogen can be done in a number of ways involving condensation, temperature or pressure swing adsorption, molecular sieve adsorbents or a combination of options (Ligen et al., 2020; Peschel, 2020). Increased interest in the energy requirements of this step result from the efficiency concerns of green hydrogen production and use. Drying has been achieved using a vacuum assisted pressure swing adsorption system with an energy requirement of 0.5 $kWh.kg^{-1}$ H_2 (Ligen et al., 2020). This system also specified a 98.4% recovery rate of hydrogen for the process and extremely low remaining moisture in the system (<ppmV, assumed to be 100% effective here).

2.7 Electrochemical Ammonia Generation

Water fed cells are constrained to those operating with liquid water rather than steam, with ambient and moderate temperatures and pressures assumed for assessment. Conditions were chosen from literature data which, in reality, shows a large range of performance outcomes with no clear connection to operational conditions. McPherson et al. (2019) showed no clear connection between rate and temperature with most results having faradaic efficiency <10%. Wu et al. (2021) showed recent results with faradaic efficiency ranging fairly evenly between 5 and 50% while a comprehensive table of both faradaic efficiency and operating conditions collated by Guo (Guo et al., 2019) also showed no connection or clear trend between performance and operating conditions, the reaction still heavily influenced by fundamental and mechanistically controlled limitations. Some evidence that increasing the temperature up to 60°C can improve both faradaic efficiency and yield considerably has been presented (Qin et al., 2018) and therefore as a conservative estimate 60°C has been used for both hydrogen and water fed cells since this is also the operational temperature of electrolysis and fuel cells and reduces process complexity. The majority of authors have not attempted to pressurise the cell, although Suryanto et al. (2021) recently presented an interesting study with increased pressure on the cathode side showing high performance. Ambient pressure is assumed here however in keeping with most approaches for electrochemical ammonia formation.

Electrical energy requirements for electrolysis are intrinsically linked to both the faradaic efficiency and the operating cell voltage through the following relationship:

$$E_S = \frac{V_{cell} \times n \times F}{3.6 \times 10^6 \times \eta_f} \tag{6}$$

Where E_S is the specific energy to form 1 mol of ammonia (kWh/mol NH_3), V_{cell} is the total cell voltage, n is the moles electrons transferred to make 1 mol of ammonia, F is Faraday's constant for the amount of charge passed when transferring an electron (96485°C mol e^{-1}) and η_f is the faradaic efficiency of the cell. The equation also includes a unit adjustment. The faradaic efficiency takes into account losses from side-reactions while the operating cell voltage includes energy losses like ohmic losses from polarisation, reaction overpotentials, diffusion limitations and other electrochemical cell specific inefficiencies. E_{cell}, as collated for hydrogen and water-fed cells in **Figure 2**, would likely be an underestimate if using half-cell potentials for ammonia formation versus the NHE since it neglects specifics of full cell arrangement such as membrane ohmic resistance. However, overpotential is still expected to be the dominant source of inefficiency in this case and gives a reasonable estimate.

For a range of applied potentials and faradaic efficiencies the specific energy consumption of electrolysis can be calculated as shown in **Figure 3**, demonstrating a large unknown boundary on this basis.

For the base case analysis, a 60% faradaic efficiency was used while $E_{cell,H2O}$ = 1.7 V and $E_{cell,H2}$ = 0.5 V (i.e. ammonia formation potential at −0.5 V vs NHE in both cases). There is often a relationship between the applied potential and the faradaic efficiency, with larger potentials showing a lower faradaic efficiency and side reactions being linked to the extent of electrode polarisation, however for this system findings of this relationship have been hugely variable and in this work they have been treated as independent process inputs, The faradaic efficiency is an important assumption since it will dictate how much hydrogen or water is required within the anode since some is consumed only to produce more hydrogen through inefficiency at the cathode. The faradaic efficiency will also determine the amount of hydrogen needed initially through the water electrolysis unit operation, as well as the post-processing at the cathode since a low faradaic efficiency will result in an increased concentration of hydrogen at the cathode requiring processing and separation from the ammonia product regardless of the arrangement. 60% has been chosen as an optimistic starting point for the system, but does have some literature precedent demonstrating it is possible to achieve (Cong et al., 2019; Wei et al., 2021).

Other important assumptions when considering a full process analysis of electrochemical systems is the conversion per pass of the reactants, also sometimes referred to as reactant utilisation. Unconverted reactants represent inefficiencies as they must be heated, cooled and separated from streams and can add significant inefficiency to the system and inflate the energy demand of the process. The Haber-Bosch itself runs with low conversion rates [20–30% hydrogen conversion (Rouwenhorst et al., 2019)] meaning the synthesis loop must handle large flow rates. Low conversion rate in addition to low faradaic conversion will exacerbate this issue in the electrochemical conversion system. Since conversions are highly dependent on the continuous cell arrangement and design, little to no information for the electrochemical ammonia system has been collected. The modelling work of Kugler et al. (2014) used conversion of 50 mol% of reactants at both the cathode and anode compartment of their water-fed model. This is similar to results found for water electrolysis and in other electrochemical devices such as fuel cells which tend to also operate at around 40–60% conversion per pass. In this work 50 mol% conversion is used with sensitivity analysis carried out on this important process variable.

2.8 Water Electrolysis (H_2-Fed Cell Only)

In the case of the H_2-fed cell, hydrogen must be generated as a feedstock for ammonia generation. Water electrolysis is heavily

studied and optimised arrangements now exist, with performance increasing as catalyst design advances. In this work, energy consumption has been taken from Carmo et al. (2013) of 4.2 kWh.Nm^{-3} H_2 produced with mid-point operating temperature of the cell at 60°C, matching the temperature of the ammonia cell. Hydrogen produced at a purity of 99.995 mol% (balance oxygen via slippage) and energy for water purification prior to introduction by reverse osmosis (RO) is also embedded into the energy demand of electrolysis as 0.003 kWh/kg water (Rouwenhorst et al., 2019) (RO requirement also embedded in the energy demand of the water-fed ammonia cell), a very small contribution to power requirements overall. Humidity of 95% was assumed for the hydrogen product stream leaving the electrolysis unit.

2.9 Hydrogen Fuel Cell (H_2O-Fed Cell Only)

With large amounts of hydrogen being produced but not used in the H_2O-fed cell, hydrogen generation represents a significant energy penalty for the H_2O-fed process. If it could be purified and directed through a fuel cell, this could potentially offset energy use for the process and has been explored here. Hydrogen utilisation (conversion per pass) was found to be as high as 82 mol% in the optimisation work done by Shen et al. (Shen et al., 2020) where a final system efficiency of 55.54% was determined at an operational temperature of 60°C. Water generated in the fuel cell was recycled here to the H_2O-fed cell, less the amount remaining in vapour form at the fuel cell output, assumed to be at 95% humidity.

2.10 Ammonia Separation (Absorption/ Desorption)

In the commercial Haber-Bosch arrangement, ammonia separation is generally achieved through pressurised refrigeration, taking reactant streams to low temperatures while retaining pressure used in the ammonia synthesis loop (Rouwenhorst et al., 2019). In the scenarios used here, atmospheric pressure is used for the reactor, meaning use of pressurised refrigeration requires post-synthesis pressurisation and energy additional to the main reactor. In this case, the absorption technique can alternatively be considered as an attractive alternative.

The absorption technique is a system modification which replaces the refrigeration condenser with dual absorption columns. This fulfils the same purpose as the condenser: as the ammonia passes over the absorbent, it is effectively being removed from the gas phase and lowering the pressure. When the absorbent is saturated, the piping switches columns so column 2 can absorb while column 1 desorbs ammonia by being heated. The absorption technique is more compatible with intermittent power, which could be a large benefit for renewable-based systems. The absorption technique was shown to significantly drop the energy required in the 0 to 24 t/d size range (Rouwenhorst et al., 2019), and cost minimised in the 100–10,000 kg/h ammonia production range (Palys et al., 2018). Modelling has not been done for integration with an electrochemical system and is usually applied to the pressurised Haber-Bosch synthesis loop. In the layout presented here, pressure must be increased prior to use of the absorption technique and the process schematic has been modified from that of Palys et al. (2018) to be added in after the electrochemical ammonia generation. The conditions specified by Palys et al. for their adsorption/recovery model have been used here. The absorber is supplied with the anode outlet at 20 bar and 167°C (after compression and heat exchange as per **Section 2.2 and 2.3**), spent gas exiting under these conditions to downstream decompression and internal recycle. The exit gas is assumed to have 5 mol% ammonia still present while the desorbed component is pure ammonia. Desorption occurs under reduced pressure and high temperature of 13 bar and 500°C. The outlet ammonia is then further compressed and cooled to obtain a liquid product at 23.4 bar and 56°C. The energy requirements for the ammonia adsorption/desorption process was provided by Palys et al. as 2.56 kWh.kg^{-1} NH_3 inlet (Palys et al., 2018). This is assumed to be electrical energy since the authors used an assumption of 100% efficiency of conversion using an electric heater for the absorption/regeneration units.

3 RESULTS AND DISCUSSION

3.1 Base Model Performance

Two options for the H_2-fed arrangement were outlined in **Section 2** where it was shown that there were two main options for handing the build-up of nitrogen in the cathode compartment. The first option is to redirect the anode outlet through the membrane separation arrangement also used for recovery of hydrogen from the cathode stream. This requires compression and cooling of the anode outlet since membrane operational requirements are different to the anode, and therefore increases energy requirements from BOP. The second option is to recover the hydrogen in a fuel cell to offset electrical energy requirements.

For the base case conditions of all three scenarios including water and hydrogen fed arrangements, overall energy demand of the process and break-down of process energy requirements shown in **Figures 6A,B**.

It can be seen for base assumptions used, the H_2O-fed cell gives the lowest overall energy demand of 22 kWh.kg NH_3^{-1}, followed by H_2-fed (1) at 26 kWh.kg NH_3^{-1} and H_2-fed (2) at 35 kWh.kg $NH_3^{-1.}$ The H_2O-fed approach also has the lowest net electrochemical energy demand, however only when the electrical energy of ammonia synthesis is offset by the fuel cell electrical energy recovery. The ammonia synthesis energy required is larger as expected, considering the increased cell voltage required (see **Figure 2B**), however combination of electrical demand for both ammonia and hydrogen production is larger in both hydrogen fed cases. Option (1) is seen to be the most desirable arrangement for the H_2-fed process. In Option 2 the large energy demand for hydrogen generation is far more dominant than the slight increase in BOP requirements to pressurise the recycle stream for hydrogen recovery in Option 1. Although a slight reduction in energy requirement from the fuel cell offset can be seen in this case, it does not make up for the increased energy demand needed to produce excess hydrogen which is then not converted to

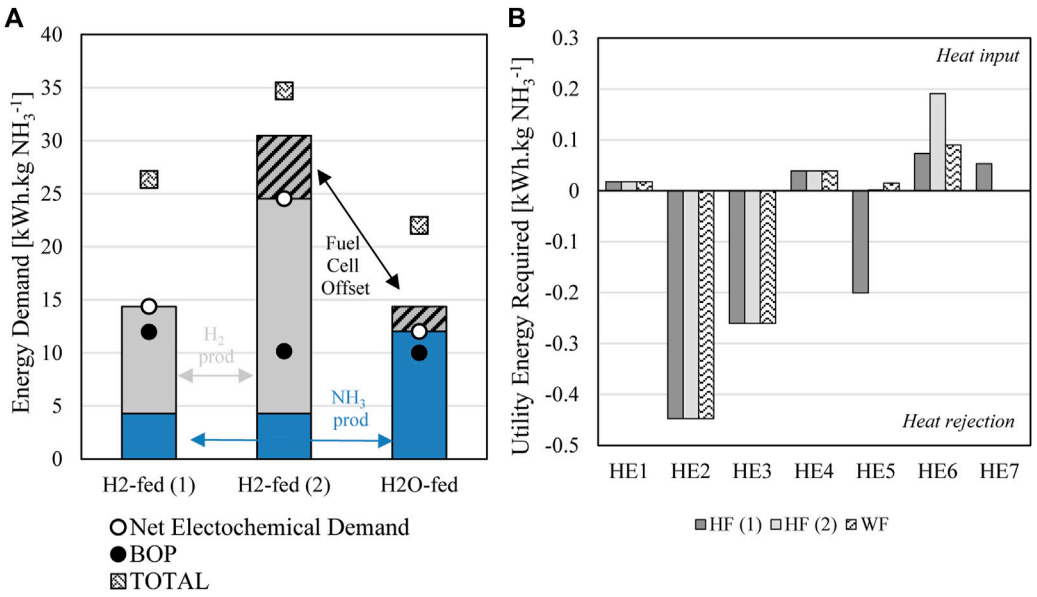

FIGURE 6 | (A) Comparison of main energy requirements for different process options **(B)** thermal energy demand (heating or cooling) for heat exchangers in each scenario as specified in **Figures 3–5**.

ammonia due to low faradaic efficiency and cell utilisation (50 mol% conversion per pass assumed in the base model scenario).

Balance of plant in all scenarios shown in **Figure 6A** includes PSA (for nitrogen production), compression, the absorption system for ammonia recovery, reverse-osmosis for water purification, condensers and hot/cold utilities after internal energy use–assumptions outlined in **Section 2**. It can be seen that BOP is similar for all arrangements, being only slightly higher in the case of H_2-fed (1). This is due to the increased compression required for recycle of the anode stream through the membrane separation.

Utility energy demand has been compared for the processes (heat exchangers specified in **Figures 3–5**) in **Figure 6B**. The utility energy requirements are small compared to the electrochemical energy demand and indeed represent a small contribution to the process. They are useful to consider to demonstrate differences between how the models operate. No difference between HE1-HE4 are seen for the models as these are located around the cathode stream where no difference in process arrangement is observed. HE5 represents cooling in the case of the H_2-fed (1), where the anode stream is compressed and then cooled to send it through the membrane separation along with the ammonia separated cathode stream. In H_2-fed (2), HE 5 is located after the membrane process to heat hydrogen to the ammonia synthesis temperature and in the water fed option it acts as the fuel cell pre-heat following membrane separation of hydrogen. HE6 is the pre-heater for all processes, bringing initial feeds up to electrolysis temperatures. It is larger for H_2-fed (2), representing the larger input required for the water electrolysis in this case to generate increased hydrogen for the single pass system. HE7 is only used for H_2-fed (1) where the hydrogen recycle stream is heated to reaction temperature following membrane separation.

It can be seen in **Figure 6B** that internal energy demand is dominated by cooling requirements, this is due to the cathode stream processing and ammonia separation where the stream must be compressed – resulting in stream heating (as per **Eq. 3**) requiring heat rejection (HE2). Following the absorber unit operation the product ammonia also requires substantial cooling (HE3). When conducting 1st and 2nd law internal

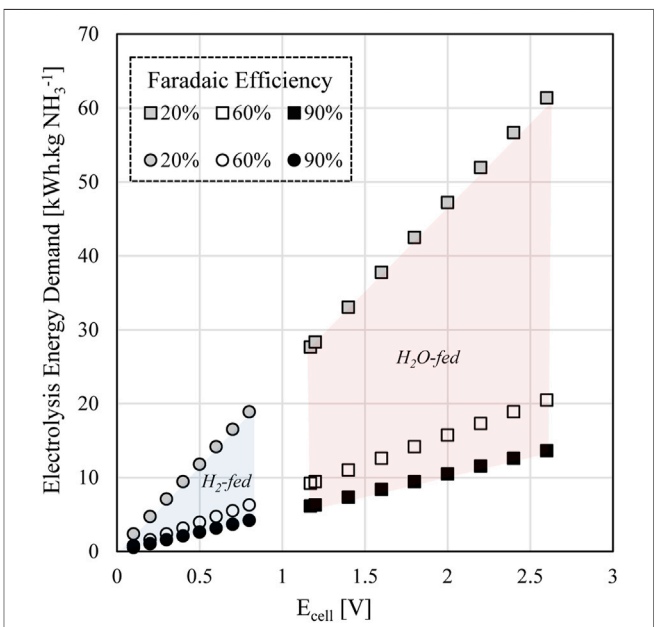

FIGURE 7 | Electrochemical energy demand for hydrogen or water fed ammonia synthesis cells depending on proton source (H_2 or H_2O) and faradaic efficinecy.

energy transfer, these low temperatures are unable to be offset by the hot streams and must necessarily be provided from a cooling utility. Overall however, utility requirements are not dominant even when considering that the final value is expected to be an underestimate of the energy requirements since inefficiencies of real unit operations compared to ideal performance will mean additional energy requirements are likely.

3.2 Sensitivity Analysis

3.2.1 Faradaic Efficiency

As discussed in **Section 2.7**, faradaic efficiency is still not optimised for ammonia synthesis, presenting a particular issue for the cathode where hydrogen is formed preferentially over ammonia. In the case of a hydrogen fed cell, this means a portion of hydrogen is consumed at the anode and reformed at the cathode, enhancing process inefficiency since additional hydrogen must be initially generated through water electrolysis. This is particularly problematic in the case where hydrogen fed through the anode is not recovered, as in the H_2-fed (2) arrangement. A comparison of total process energy demands for faradaic efficiency between 20 and 90% of the ammonia synthesis electrolyser are shown in **Figure 7**.

It can be seen in **Figure 7** that the water fed and hydrogen fed cells perform similarly when the hydrogen fed cell includes a recycle stream at the anode. The water fed option shows slightly improved outcomes at high faradaic efficiency however there is less difference at lower FE. This is reflective of the higher cell potential of the water fed cell balanced by increased BOP requirements for the hydrogen fed cell. In the hydrogen fed scenario the lower efficiency of ammonia formation does not have as great an impact on electrochemical demand as the bulk of this is carried out via water electrolysis. Energy is required to split water into hydrogen originally in the water electrolyser, and this is operating at a fixed efficiency in the current model (see **Section 2.8** for operating assumptions). The hydrogen is then transformed into ammonia using smaller energy than a direct input of water and this is also the unit operation where efficiency has been varied. In the water fed all work to form ammonia is carried out in the electrochemical ammonia generation unit and the whole electrochemical energy demand will therefore be more sensitive to changes in faradaic efficiency.

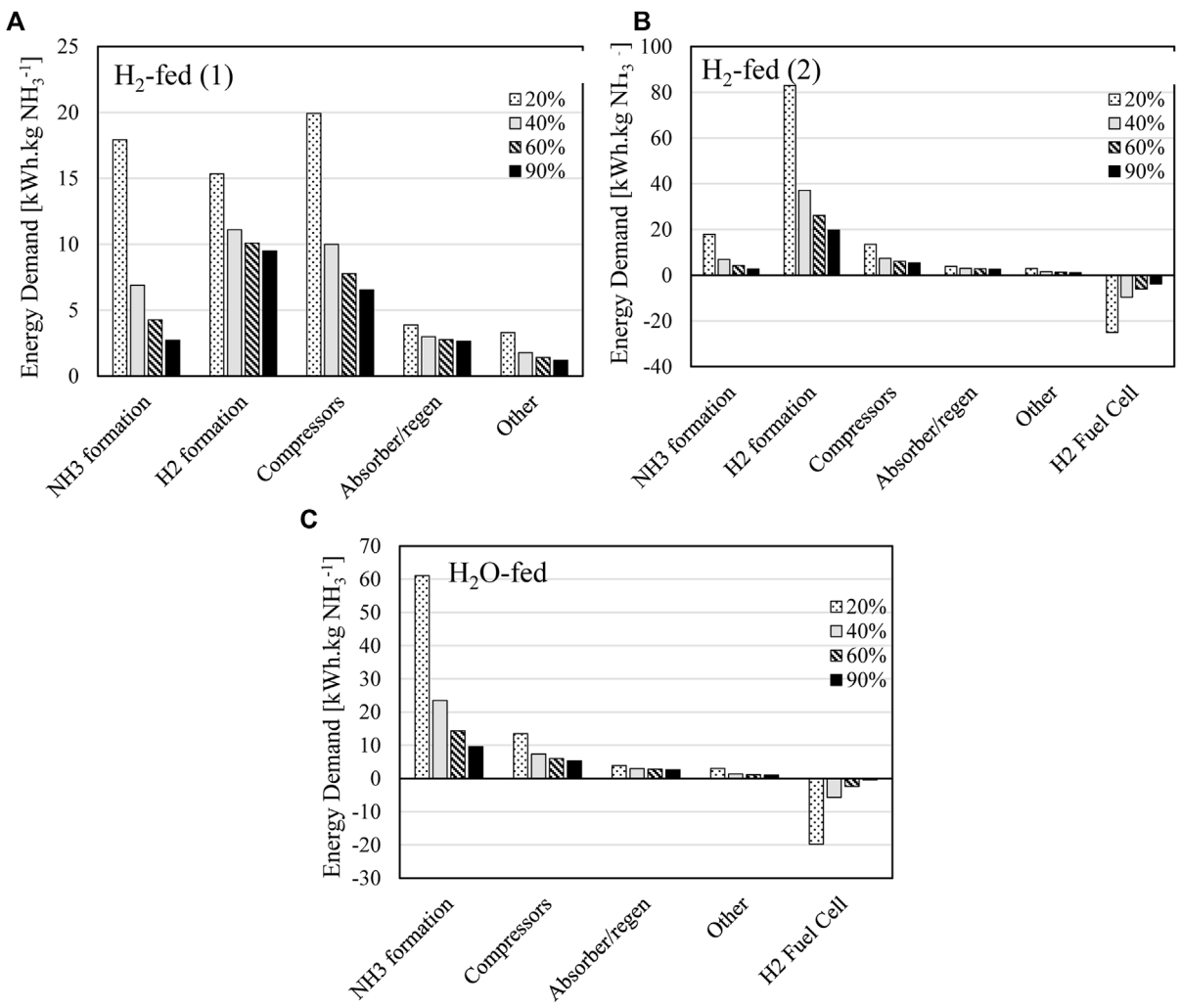

FIGURE 8 | Energy demand breakdown of different plant components for **(A)** H_2-fed (1), **(B)** H_2-fed (2), and **(C)** H_2O-fed.

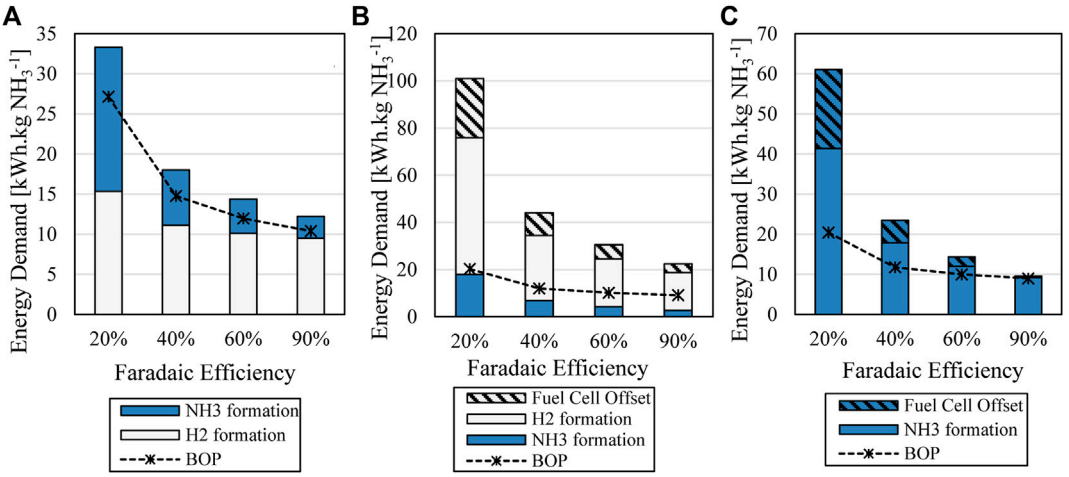

FIGURE 9 | Breakdown of electrochemical energy demand of process and combined BOP energy demand for **(A)** H_2-fed (1), **(B)** H_2-fed (2) and **(C)** H_2O-fed.

The hydrogen fed options show the advantage of H_2-fed (1) in recycling hydrogen generated. The loss of energy when hydrogen is not recycled at the anode in H_2-fed (2) is seen here, despite the increased compression requirements of H_2-fed (1), which can be clearly seen in **Figure 8A** where a breakdown of energy demands for all process options is shown.

'Other' as shown in **Figure 8** includes a combination of the smallest unit contributions including the utility requirements, condensers and PSA for nitrogen production. It can be seen that the dominant BOP energy requirement in all cases is the separation of ammonia, which encompasses the bulk of compression (in most scenarios) and absorption/regeneration.

In the case of the H_2–fed (1) cell however, the compression energy demand increases past the electrochemical demand in the case of low faradaic efficiency, and this increase is not directly related to the ammonia compression but rather the recycle requirements of hydrogen in this case. This is because decreasing the faradaic efficiency increases the hydrogen consumed at the anode for the same ammonia output. This increases the overall demand of hydrogen generation and therefore the amount of hydrogen recycled through the compression loop out of the anode. H_2-fed (2) of the hydrogen fed cell is dominated by the hydrogen generation requirement since hydrogen is not recycled at the anode at all, while ammonia formation is the largest demand for the H_2O-fed cell. This is also a result of the larger cell potential of the H_2O-fed cell (1.85 V assumed here, see **Section 2.7**) which is directly related to the energy demand via **Eq. 6**. When comparing the combined BOP energy demand for each arrangement, seen in **Figure 9**, it is most evenly matched to net electrochemical demand in the case of the H_2-fed (1) arrangement due to the additional compression requirements.

For H_2-fed (1) BOP demand increases along with the electrochemical demand as faradaic efficiency decreases, whereas in H_2-fed (2) and the H_2O-fed the BOP requirements do not increase with the same matched intensity. The BOP has the smallest impact on the H_2-fed (2) scenario, however this is due to the massive energy demand of the inefficient process arrangement. In fact, the BOP required is at a minimum for high faradaic efficiency in both the H_2O-fed and H_2-fed (1) options at 90% efficiency where the two also have closely comparable total energy demand (**Figure 10**). Importantly, the BOP still contributes significant energy demand in these cases. Previous works which have compared energy demand for electrochemical ammonia generation by ignoring BOP requirements are therefore significantly underestimating the expected energy inputs for this process, by as much as 50% as shown here, even in the case of high faradaic efficiency.

3.2.2 Conversion/Utilisation

As discussed in **Section 2.7**, the conversion of reactants as they travel through electrochemical reactors is not known for

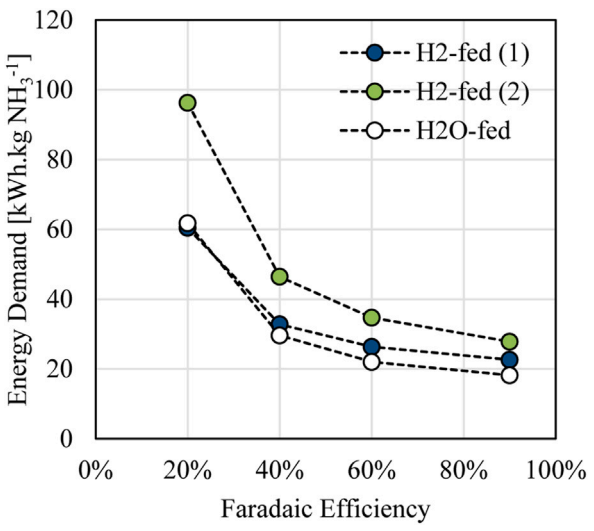

FIGURE 10 | Energy demand for different process options dependant on the faradaic efficiency.

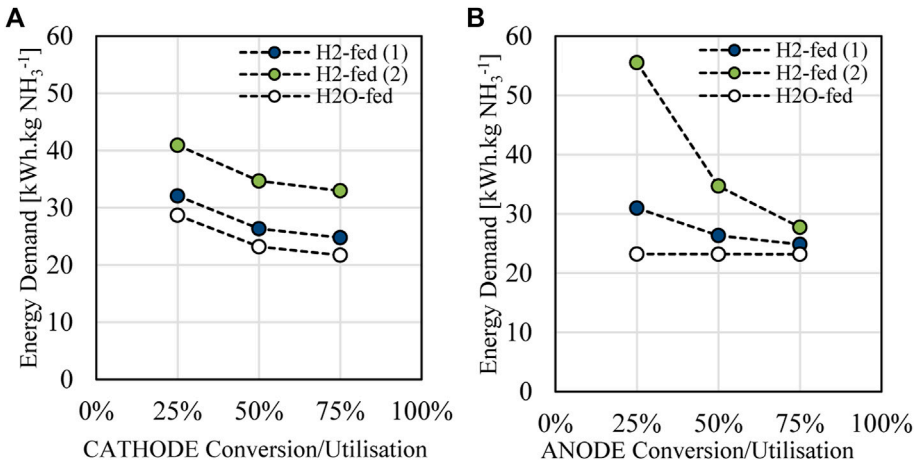

FIGURE 11 | Conversion/utilisation (in mol% of inlet reactants) impact on total process energy demand for **(A)** cathode and **(B)** anode conversion.

ammonia electrolysis due to the early stage of the technology development. 50 mol% (of inlet reactant) is thought to be reasonable compared to other electrochemical cells such as water electrolysis and gas-fed fuel cells (Carmo et al., 2013; Shen et al., 2020). Since the anode and cathode of each reactor considered here will have different impacts on the overall process demand, depending on downstream processing, the variation of conversion on both the anode and cathode component of the ammonia synthesis cell has been considered with results shown for the overall energy demand shown in **Figure 11A**.

Anode conversion is seen to have varying impacts on the energy demand depending on the cell arrangement while cathode conversion shows no difference in changes observed between the cells. Cathode conversion related to nitrogen conversion and the amount of nitrogen converted when it passes through the electrolysis unit operation. Since the cathode side of each cell is identical, similar response to conversion change would be expected as seen here (**Figure 11A**). Energy demands increase when conversion drops to 25 wt%, related to increased nitrogen generation from PSA as well as flow on effects to compression of reactor outlets and utility requirements in treatment of increased steam flows.

Greater difference in response is seen for anode conversion where in the case of the H_2O-fed cell only very slight change in energy demand is observed. This is because the anode of the water-fed cell is fully recycled through water reclamation which also is assumed to remain at the reaction temperature before being cycled, adding no additional BOP load. In reality, some increase in energy would be observed from increased pumping and unit operation energy losses, however as seen with energy utility consideration here (**Figure 6B**) this is not expected to be a dominant usage figure. In the cases where imperfect recycle is observed, i.e. H_2-fed (1), an increase in energy is required mostly due to the increased energy demand for compression of the unreacted stream following the ammonia synthesis reactor. Energy demand for the H_2-fed (2) scenario is dominated again by electrochemical generation of hydrogen, similarly to the impacts of faradaic efficiency, since a large amount of unreacted hydrogen must be produced which is not fully recovered.

3.2.3 Optimised Performance

From an energy perspective, water fed cells are the preferred method for electrochemical ammonia synthesis. Hydrogen fed cells would become more attractive if they were able to achieve greater efficiency and conversion than water fed. They might also be more attractive options in the case where ammonia formation rate of hydrogen fed cells was significantly higher than water-fed, although there is no evidence that this is the case.

A highly optimised scenario for the water fed cell includes the following assumptions: 90% faradaic efficiency, 75% anode utilisation and a cell potential of 1.5 V. Under these conditions it is possible to reduce the water fed cell to an energy demand of 15 kWh/kg NH_3. This is still larger than commercial ammonia operations, however it is possible on much smaller scales, which are not achievable when using the Haber-Bosch approach.

For the hydrogen fed arrangement, a similar value is not achieved even when both nitrogen and hydrogen utilisation at anode and cathode are as high at 75%. The optimised scenario in this case has an energy demand of 19 kWh/kg NH_3 at 90% faradaic efficiency and 0.5 V cell potential.

In this work a case study considering aqueous systems has been addressed, which has provided important insight into balance of plant sensitivities and the need to include energy demand of these components when reporting on power to ammonia values. Future investigations should consider additional process arrangements for their ability to drive down the process energy demand. For example, increasing the faradaic efficiency of the process is key to achieving low energy demand due to the flow on effect observed here for the balance of plant energy demands and is likely to outweigh energy trade-offs such as high cell voltage as seen in recent breakthroughs in the electrochemical ammonia field (Suryanto et al., 2021). Understanding all process requirements for direct electrochemical ammonia can help direct research efforts and work outlined here should be expanded on for other electrochemical systems such as aprotic and redox mediated approaches.

4 CONCLUSION

Energy demands for electrochemical ammonia generation have been calculated for three process arrangements and comparison of water or hydrogen fed synthesis approaches carried out. It can be seen that balance of plant (BOP) requirements for electrochemical ammonia synthesis are significant and could influence the selection of technology pathways in future decarbonisation scenarios. Energy demands of compression and ammonia separation are significant compared to electrical inputs for the synthesis reactor, particularly at high faradaic efficiency. In the most efficient set up, BOP demands account for nearly 50% of plant energy demands, mostly in ammonia separation and an energy demand of 15 kWh.kg NH_3^{-1}. It is therefore shown here that comparing energy requirements of electrochemical synthesis only, using the energy demands of the electrochemical reactor, is only part of the expected consumption. It has also been shown that efficient recycle of anode outputs is key in the case of hydrogen fed cells. At low conversion or faradaic efficiency, energy demand for separation of hydrogen and nitrogen mixtures becomes of great significance. It was further found that although ammonia synthesis from hydrogen feeds has a lower cell potential, the combination of both hydrogen generation and ammonia synthesis result in higher overall energy demand compared to direct ammonia synthesis using water as a proton source in the base case analysed, 26 kWh/kg NH_3^{-1} compared to 22 kWh/kg NH_3^{-1}. Breaking the reaction into two steps introduces a source of inefficiency which is not overcome by reduced BOP energy demands, and will only be an attractive pathway for reactors which promise both high efficiency and increased ammonia formation rate compared to water fed cells.

DATA AVAILABILITY STATEMENT

The raw data supporting the conclusions of this article will be made available by the authors, without undue reservation.

AUTHOR CONTRIBUTIONS

JA contributed to the conception and design of the study, SP contributed to the process design, built the initial model and collated information which was included in the work, JA wrote the first draft of the manuscript, built the final model and conducted analysis on outcomes, SP wrote sections of the manuscript, all authors contributed to manuscript revision, read, and approved the submitted version.

FUNDING

JA acknowledges funding from the Australian Research Council provided during the preparation of this work under grant DE210100680.

SUPPLEMENTARY MATERIAL

The Supplementary Material for this article can be found online at: https://www.frontiersin.org/articles/10.3389/fceng.2021.765457/full#supplementary-material

REFERENCES

Allen, J. A., Glenn, M., and Donne, S. W. (2020). Analysis of Theoretical Efficiency in a Model 10 kW Direct Carbon Fuel Cell Using a Coal Based Carbonate Slurry. *Electrochimica Acta* 329, 135131. doi:10.1016/j.electacta.2019.135131

Amar, I., Lan, R., Petit, C. T. G., and Tao, S. (2010). Solid-state Electrochemical Synthesis of Ammonia: A Review. *J. Solid State. Electrochemistry* 15, 1845–1860. doi:10.1007/s10008-011-1376-x

Boerner, L. (2019). Industrial Ammonia Production Emits More CO_2 Than Any Other Chemical-Making Reaction. *Chem. Eng. News* 97 (24), 1–9.

Carmo, M., Fritz, D. L., Mergel, J., and Stolten, D. (2013). A Comprehensive Review on PEM Water Electrolysis. *Int. J. Hydrogen Energ.* 38 (12), 4901–4934. doi:10.1016/j.ijhydene.2013.01.151

Chehade, G., and Dincer, I. (2021). Advanced Kinetic Modelling and Simulation of a New Small Modular Ammonia Production Unit. *Chem. Eng. Sci.* 236, 116512. doi:10.1016/j.ces.2021.116512

Cherepanov, P. V., Krebsz, M., Hodgetts, R. Y., Simonov, A. N., and MacFarlane, D. R. (2021). Understanding the Factors Determining the Faradaic Efficiency and Rate of the Lithium Redox-Mediated N2 Reduction to Ammonia. *J. Phys. Chem. C* 125 (21), 11402–11410. doi:10.1021/acs.jpcc.1c02494

Choi, J., Suryanto, B. H. R., Wang, D., Du, H.-L., Hodgetts, R. Y., Ferrero Vallana, F. M., et al. (2020). Identification and Elimination of False Positives in Electrochemical Nitrogen Reduction Studies. *Nat. Commun.* 11 (1), 5546. doi:10.1038/s41467-020-19130-z

Cong, L., Yu, Z., Liu, F., and Huang, W. (2019). Electrochemical Synthesis of Ammonia from N2 and H2O Using a Typical Non-noble Metal Carbon-Based Catalyst under Ambient Conditions. *Catal. Sci. Technol.* 9 (5), 1208–1214. doi:10.1039/c8cy02316f

David, O. C., Gorri, D., Urtiaga, A., and Ortiz, I. (2011). Mixed Gas Separation Study for the Hydrogen Recovery from H2/CO/N2/CO2 post Combustion Mixtures Using a Matrimid Membrane. *J. Membr. Sci.* 378 (1), 359–368. doi:10.1016/j.memsci.2011.05.029

David, O. C., Gorri, D., Nijmeijer, K., Ortiz, I., and Urtiaga, A. (2012). Hydrogen Separation from Multicomponent Gas Mixtures Containing CO, N2 and CO2 Using Matrimid Asymmetric Hollow Fiber Membranes. *J. Membr. Sci.* 419-420, 49–56. doi:10.1016/j.memsci.2012.06.038

Don, W. G., and Robert, H. P. (2008). *Perry's Chemical Engineers' Handbook*. Eighth Edition8th ed./. New York: McGraw-Hill Education.

Erisman, J. W., Sutton, M. A., Galloway, J., Klimont, Z., and Winiwarter, W. (2008). How a century of Ammonia Synthesis Changed the World. *Nat. Geosci* 1 (10), 636–639. doi:10.1038/ngeo325

Giddey, S., Badwal, S. P. S., and Kulkarni, A. (2013). Review of Electrochemical Ammonia Production Technologies and Materials. *Int. J. Hydrogen Energ.* 38 (34), 14576–14594. doi:10.1016/j.ijhydene.2013.09.054

Guo, W., Zhang, K., Liang, Z., Zou, R., and Xu, Q. (2019). Electrochemical Nitrogen Fixation and Utilization: Theories, Advanced Catalyst Materials and System Design. *Chem. Soc. Rev.* 48 (24), 5658–5716. doi:10.1039/c9cs00159j

Han, J., Liu, Z., Ma, Y., Cui, G., Xie, F., Wang, F., et al. (2018). Ambient N2 Fixation to NH3 at Ambient Conditions: Using Nb2O5 Nanofiber as a High-Performance Electrocatalyst. *Nano Energy* 52, 264–270. doi:10.1016/j.nanoen.2018.07.045

Kemp, I. C. (2011). *Pinch Analysis and Process Integration: A User Guide on Process Integration for the Efficient Use of Energy*. Elsevier.

Kordali, V., Kyriacou, G., and Lambrou, C. (2000). Electrochemical Synthesis of Ammonia at Atmospheric Pressure and Low Temperature in a Solid Polymer Electrolyte Cell. *Chem. Commun.* 2000 (17), 1673–1674. doi:10.1039/b004885m

Kugler, K., Ohs, B., Scholz, M., and Wessling, M. (2014). Towards a Carbon Independent and CO2-free Electrochemical Membrane Process for NH3 Synthesis. *Phys. Chem. Chem. Phys.* 16 (13), 6129–6138. doi:10.1039/c4cp00173g

Kyriakou, V., Garagounis, I., Vasileiou, E., Vourros, A., and Stoukides, M. (2017). Progress in the Electrochemical Synthesis of Ammonia. *Catal. Today* 286, 2–13. doi:10.1016/j.cattod.2016.06.014

Lan, R., Irvine, J. T. S., and Tao, S. (2013). Synthesis of Ammonia Directly from Air and Water at Ambient Temperature and Pressure. *Sci. Rep.* 3 (1), 1145. doi:10.1038/srep01145

Ligen, Y., Vrubel, H., and Girault, H. (2020). Energy Efficient Hydrogen Drying and Purification for Fuel Cell Vehicles. *Int. J. Hydrogen Energ.* 45 (18), 10639–10647. doi:10.1016/j.ijhydene.2020.02.035

MacFarlane, D. R., Cherepanov, P. V., Choi, J., Suryanto, B. H. R., Hodgetts, R. Y., Bakker, J. M., et al. (2020). A Roadmap to the Ammonia Economy. *Joule* 4 (6), 1186–1205. doi:10.1016/j.joule.2020.04.004

McPherson, I. J., Sudmeier, T., Fellowes, J., and Tsang, S. C. E. (2019). Materials for Electrochemical Ammonia Synthesis. *Dalton Trans.* 48 (5), 1562–1568. doi:10.1039/c8dt04019b

Nazemi, M., Ou, P., Alabbady, A., Soule, L., Liu, A., Song, J., et al. (2020). Electrosynthesis of Ammonia Using Porous Bimetallic Pd-Ag Nanocatalysts in Liquid- and Gas-phase Systems. *ACS Catal.* 10 (17), 10197–10206. doi:10.1021/acscatal.0c02680

Palys, M., McCormick, A., Cussler, E., and Daoutidis, P. (2018). Modeling and Optimal Design of Absorbent Enhanced Ammonia Synthesis. *Processes* 6 (7), 91. doi:10.3390/pr6070091

Peschel, A. (2020). Industrial Perspective on Hydrogen Purification, Compression, Storage, and Distribution. *Fuel Cells* 20 (4), 385–393. doi:10.1002/fuce.201900235

Qin, Q., Heil, T., Antonietti, M., and Oschatz, M. (2018). Single-Site Gold Catalysts on Hierarchical N-Doped Porous Noble Carbon for Enhanced Electrochemical Reduction of Nitrogen. *Small Methods* 2 (12), 1800202. doi:10.1002/smtd.201800202

Ritchie, H., and Roser, M. (2020). *CO_2 and Greenhouse Gas Emissions*.

Rouwenhorst, K. H. R., Van der Ham, A. G. J., Mul, G., and Kersten, S. R. A. (2019). Islanded Ammonia Power Systems: Technology Review & Conceptual Process Design. *Renew. Sust. Energ. Rev.* 114, 109339. doi:10.1016/j.rser.2019.109339

Sánchez, A., and Martín, M. (2018). Scale up and Scale Down Issues of Renewable Ammonia Plants: Towards Modular Design. *Sustainable Prod. Consumption* 16, 176–192. doi:10.1016/j.spc.2018.08.001

Schell, W. J. (1985). Commercial Applications for Gas Permeation Membrane Systems. *J. Membr. Sci.* 22 (2), 217–224. doi:10.1016/s0376-7388(00)81281-8

Shen, K.-Y., Park, S., and Kim, Y.-B. (2020). Hydrogen Utilization Enhancement of Proton Exchange Membrane Fuel Cell with Anode Recirculation System through a Purge Strategy. *Int. J. Hydrogen Energ.* 45 (33), 16773–16786. doi:10.1016/j.ijhydene.2020.04.147

Shipman, M. A., and Symes, M. D. (2017). Recent Progress towards the Electrosynthesis of Ammonia from Sustainable Resources. *Catal. Today* 286, 57–68. doi:10.1016/j.cattod.2016.05.008

Singh, A. R., Rohr, B. A., Schwalbe, J. A., Cargnello, M., Chan, K., Jaramillo, T. F., et al. (2017). Electrochemical Ammonia Synthesis-The Selectivity Challenge. *ACS Catal.* 7 (1), 706–709. doi:10.1021/acscatal.6b03035

Smith, C., Hill, A. K., and Torrente-Murciano, L. (2020). Current and Future Role of Haber-Bosch Ammonia in a Carbon-free Energy Landscape. *Energy Environ. Sci.* 13 (2), 331–344. doi:10.1039/c9ee02873k

Suryanto, B. H. R., Matuszek, K., Choi, J., Hodgetts, R. Y., Du, H.-L., Bakker, J. M., et al. (2021). Nitrogen Reduction to Ammonia at High Efficiency and Rates Based on a Phosphonium Proton Shuttle. *Science* 372 (6547), 1187–1191. doi:10.1126/science.abg2371

Tang, C., and Qiao, S.-Z. (2019). How to Explore Ambient Electrocatalytic Nitrogen Reduction Reliably and Insightfully. *Chem. Soc. Rev.* 48 (12), 3166–3180. doi:10.1039/c9cs00280d

Tao, H., Choi, C., Ding, L.-X., Jiang, Z., Han, Z., Jia, M., et al. (2019). Nitrogen Fixation by Ru Single-Atom Electrocatalytic Reduction. *Chem* 5 (1), 204–214. doi:10.1016/j.chempr.2018.10.007

Wei, X., Pu, M., Jin, Y., and Wessling, M. (2021). Efficient Electrocatalytic N2 Reduction on Three-phase Interface Coupled in a Three-Compartment Flow Reactor for the Ambient NH3 Synthesis. *ACS Appl. Mater. Inter.* 13 (18), 21411–21425. doi:10.1021/acsami.1c03698

Wu, T., Fan, W., Zhang, Y., and Zhang, F. (2021). Electrochemical Synthesis of Ammonia: Progress and Challenges. *Mater. Today Phys.* 16, 100310. doi:10.1016/j.mtphys.2020.100310

Xue, X., Chen, R., Yan, C., Zhao, P., Hu, Y., Zhang, W., et al. (2019). Review on Photocatalytic and Electrocatalytic Artificial Nitrogen Fixation for Ammonia Synthesis at Mild Conditions: Advances, Challenges and Perspectives. *Nano Res.* 12 (6), 1229–1249. doi:10.1007/s12274-018-2268-5

Yang, J., Weng, W., and Xiao, W. (2020). Electrochemical Synthesis of Ammonia in Molten Salts. *J. Energ. Chem.* 43, 195–207. doi:10.1016/j.jechem.2019.09.006

Yang, X., Nash, J., Anibal, J., Dunwell, M., Kattel, S., Stavitski, E., et al. (2018). Mechanistic Insights into Electrochemical Nitrogen Reduction Reaction on Vanadium Nitride Nanoparticles. *J. Am. Chem. Soc.* 140 (41), 13387–13391. doi:10.1021/jacs.8b08379

Yoshida, M., Ogawa, T., Imamura, Y., and Ishihara, K. N. (2021). Economies of Scale in Ammonia Synthesis Loops Embedded with Iron- and Ruthenium-Based Catalysts. *Int. J. Hydrogen Energ.* 46 (57), 28840–28854. doi:10.1016/j.ijhydene.2020.12.081

Zhou, F., Azofra, L. M., Ali, M., Kar, M., Simonov, A. N., McDonnell-Worth, C., et al. (2017). Electro-synthesis of Ammonia from Nitrogen at Ambient Temperature and Pressure in Ionic Liquids. *Energ. Environ. Sci.* 10 (12), 2516–2520. doi:10.1039/c7ee02716h

Conflict of Interest: Author AB is employed by Restech and SP received a scholarship stipend from the company for participating in this project.

The remaining author declares that the research was conducted in the absence of any commercial or financial relationships that could be construed as a potential conflict of interest.

Publisher's Note: All claims expressed in this article are solely those of the authors and do not necessarily represent those of their affiliated organizations, or those of the publisher, the editors and the reviewers. Any product that may be evaluated in this article, or claim that may be made by its manufacturer, is not guaranteed or endorsed by the publisher.